

# Current-Induced Switching of Perpendicularly Magnetized Magnetic Layers Using Spin Torque from the Spin Hall Effect

Luqiao Liu,<sup>1</sup> O. J. Lee,<sup>1</sup> T. J. Gudmundsen,<sup>1</sup> D. C. Ralph,<sup>1,2</sup> and R. A. Buhrman<sup>1</sup>

<sup>1</sup>Cornell University, Ithaca, New York 14853, USA

<sup>2</sup>Kavli Institute at Cornell, Ithaca, New York, 14853

(Received 24 April 2012; published 29 August 2012)

We show that in a perpendicularly magnetized Pt/Co bilayer the spin-Hall effect (SHE) in Pt can produce a spin torque strong enough to efficiently rotate and switch the Co magnetization. We calculate the phase diagram of switching driven by this torque, finding quantitative agreement with experiments. When optimized, the SHE torque can enable memory and logic devices with similar critical currents and improved reliability compared to conventional spin-torque switching. We suggest that the SHE torque also affects current-driven magnetic domain wall motion in Pt/ferromagnet bilayers.

DOI: 10.1103/PhysRevLett.109.096602

PACS numbers: 72.25.Ba, 72.25.Mk, 72.25.Rb, 76.50.+g

Several experiments have shown recently that an in-plane current can influence or even directly control the magnetization dynamics in a ferromagnet–heavy-metal bilayer for heavy metals such as Pt or Ta [1–12]. Two different mechanisms have been proposed. For in-plane-polarized magnetic films, spin currents arising from the spin-Hall effect (SHE) [13–20] within the heavy metal have been shown to apply spin-transfer torques to the magnet that can explain current-induced tuning of magnetic damping [1,3–5] and spin wave attenuation [6,7], and the excitation of spin wave oscillations [2], magnetic precession [3], and switching [8]. In contrast, for perpendicularly polarized magnetic layers, Rashba effects within the magnetic layer have been proposed as the dominant mechanism for current-induced magnetic tilting and reversal [9–12]. Here we show that rotation and switching of perpendicularly polarized Pt/Co driven by an in-plane current can be explained quantitatively by spin torque (ST) from the SHE, with the same SHE strength found for in-plane-polarized samples [3,21], and with no measurable Rashba field. We estimate that the SHE torque should be capable of manipulating perpendicularly polarized magnetic memory devices using switching currents that are comparable to conventional spin-transfer-torque magnetic tunnel junctions [22], so that SHE-torque switching could be highly effective for technologies.

We will analyze magnetic rotation and switching driven by an in-plane current for perpendicularly polarized Pt(20)/Co(6)/AlO<sub>x</sub> multilayers (thicknesses in Å), similar to observations by Miron *et al.* [11]. Figures 1(a) and 1(b) show switching for a device patterned into a Hall bar with dimensions 20 × 200 μm<sup>2</sup> [Fig. 1(c)], with a resistance of ~2000 Ω. We measure the anomalous Hall resistance  $R_H$ , which is proportional to the average vertical component of the Co magnetization  $M_z$  [23]. Measurements as a function of a vertical magnetic field near zero current establish the existence of perpendicular magnetic anisotropy [Fig. 1(d)]. In Fig. 1(a) we apply a small constant in-plane magnetic

field (along the current direction  $\hat{y}$  shown in Fig. 1(e), i.e.,  $\beta = 0^\circ$ ) that tilts the average moment by approximately  $2^\circ$  from vertical, but does not provide any preference for either the up or down magnetic state in the absence of the current. With no change in the direction of this fixed field, sweeping a quasistatic in-plane current then

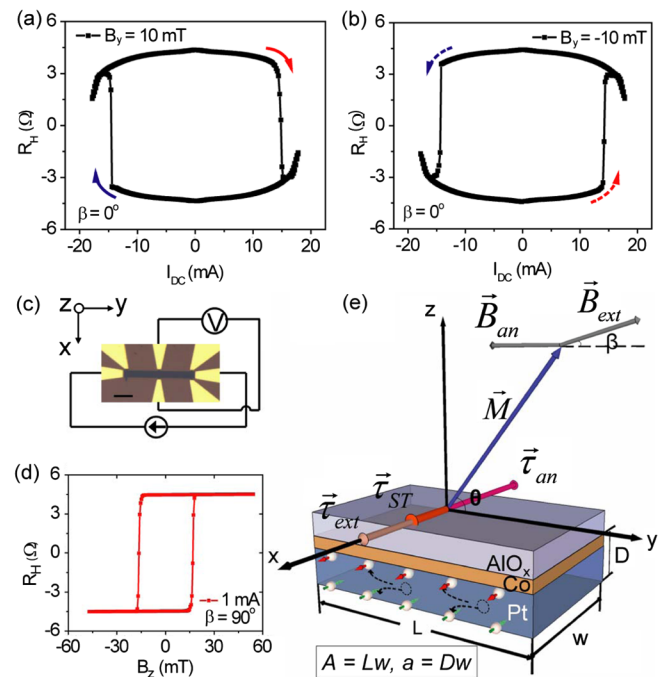


FIG. 1 (color online). (a), (b) Current-induced switching in a Pt/Co/AlO<sub>x</sub> sample at room temperature in the presence of a small, fixed in-plane magnetic field  $B_y$  with (a)  $B_y = 10$  mT and (b)  $B_y = -10$  mT. (c) Top view of the sample (50 μm scale bar). (d)  $R_H$  as a function of  $B_{ext}$  perpendicular to the sample plane. (e) Illustration of the torques exerted by the external field  $\vec{B}_{ext}$ , the anisotropy field  $\vec{B}_{an}$ , and the SHE torque  $\vec{\tau}_{ST}$  for positive current, when  $\vec{B}_{ext}$  and  $\vec{M}$  are in the  $yz$  plane. The dashed arrows show the direction of electron flow for positive current.

generates hysteretic magnetic switching between the  $M_z > 0$  and  $M_z < 0$  states, with the positive current favoring  $M_z < 0$  [Fig. 1(a)]. If the small constant in-plane magnetic field is reversed, the current-driven transitions invert, with the positive current now favoring  $M_z > 0$ , despite the fact that the in-plane field still does not favor either magnetic state in the absence of a current [Fig. 1(b)]. The current-generated Oersted magnetic field cannot explain this result, as it is oriented in-plane. We will show that the full switching phase diagram as a function of the current and magnetic field can be explained quantitatively by SHE torque from the Pt layer, and that previously proposed Rashba effects within the Co [9,11] do not make any measurable contribution to the magnetic orientation in our samples.

*Phase diagram of a macrospin model.*—To explain how a SHE torque can rotate and switch the magnetic orientation  $\hat{m}$  of a perpendicularly magnetized layer, we first solve a simple zero-temperature macrospin model. We consider a Co/Pt bilayer in the  $xy$  plane with a Co layer of thickness  $t$  and constant magnetization  $M_S$ , on top of a Pt layer of thickness  $d$  [Fig. 1(e)]. For positive current (electrons flowing in the  $-\hat{y}$  direction) the SHE induces a spin current density  $(\hbar/2)J_S/e$  within the Pt layer such that spin moments pointing in the  $\hat{\sigma} = \hat{x}$  direction (spin angular momentum along  $-\hat{x}$ ) flow upward in the  $\hat{z}$  direction. At the Pt/ferromagnet interface, the spin component perpendicular to  $\hat{m}$  can be absorbed by the ferromagnet, imparting a spin-transfer “torque” per unit moment  $\vec{\tau}_{ST} = \tau_{ST}^0(\hat{m} \times \hat{\sigma} \times \hat{m}) = \frac{\hbar}{2eM_S t} J_S(\hat{m} \times \hat{\sigma} \times \hat{m})$ , oriented along  $\hat{x}$ . We will analyze the case of an applied magnetic field  $\vec{B}_{\text{ext}} = 0\hat{x} + B_y\hat{y} + B_z\hat{z}$  (the model is generalizable to arbitrary directions). In addition to the spin torque, we must also take into account the torques (per unit moment) due to the external magnetic field,  $\vec{\tau}_{\text{ext}} = -\hat{m} \times \vec{B}_{\text{ext}}$ , and the perpendicular anisotropy field,  $\vec{\tau}_{\text{an}} = -\hat{m} \times \vec{B}_{\text{an}} = -\hat{m} \times [-B_{\text{an}}^0(\hat{m} - m_z\hat{z})] = -\hat{m} \times [B_{\text{an}}^0 m_z\hat{z}]$ . The equilibrium orientations of  $\hat{m}$  satisfy the condition  $\vec{\tau}_{\text{tot}} = \vec{\tau}_{ST} + \vec{\tau}_{\text{ext}} + \vec{\tau}_{\text{an}} = 0$ . We use macrospin simulations of the equation of motion [24]  $(1/|\gamma|)d\hat{m}/dt = \vec{\tau}_{\text{tot}} + (\alpha/|\gamma|)\hat{m} \times (d\hat{m}/dt)$  with  $\alpha > 0$  to distinguish stable from unstable equilibria.

For currents corresponding to small to moderate values of spin torque,  $|\tau_{ST}^0| < 0.5B_{\text{an}}^0$ ,  $\hat{m}$  can remain within the  $yz$  plane as long as  $B_x = 0$ . In this case all three torques ( $\vec{\tau}_{ST}$ ,  $\vec{\tau}_{\text{ext}}$ ,  $\vec{\tau}_{\text{an}}$ ) are collinear in the  $\hat{x}$  direction and the torque balance equation that determines the magnetization rotation angle  $\theta$  takes a simple scalar form,

$$\begin{aligned} \tau_{\text{tot}} &\equiv \hat{x} \cdot (\vec{\tau}_{ST} + \vec{\tau}_{\text{ext}} + \vec{\tau}_{\text{an}}) \\ &= \tau_{ST}^0 + B_{\text{ext}} \sin(\theta - \beta) - B_{\text{an}}^0 \sin\theta \cos\theta = 0, \end{aligned} \quad (1)$$

with  $\theta$  and the applied field angle  $\beta$  defined as in Fig. 1(e) with  $-\pi/2 < \beta \leq \pi/2$ . As the current is ramped from zero for fixed  $\vec{B}_{\text{ext}}$ , the dominant effect of  $\vec{\tau}_{ST}$  is to rotate  $\hat{m}$  within the  $yz$  plane, shifting  $\theta$  continuously, until, for

sufficiently large currents (relative to the anisotropy strength), Eq. (1) predicts abrupt hysteretic switching. In Fig. 2(a) we show magnetic hysteresis curves predicted by this macrospin model for fixed in-plane magnetic fields. Just as observed experimentally [Figs. 1(a) and 1(b)], the sign of the hysteresis reverses when the in-plane field component is reversed. The reason for this reversal is that although an in-plane magnetic field does not favor either magnetic orientation by itself, an in-plane field breaks the symmetry in the response to the SHE torque. With a magnetic field in the in-plane  $\hat{y}$  direction, the barrier against clockwise rotation of  $\hat{m}$  from the  $m_z > 0$  to the  $m_z < 0$  state is different than for clockwise rotation from the  $m_z < 0$  to the  $m_z > 0$  state, with the result that the direction of the in-plane field determines which out-of-plane magnetic orientation will be favored by a given sign of SHE torque [Fig. 2(b)].

For very large spin torques,  $|\tau_{ST}^0| > B_{\text{an}}^0/2$ , the SHE torque is greater than the maximum restoring torque from the magnetic anisotropy  $|\vec{\tau}_{\text{an}}|$ , and for sufficiently small  $|B_{\text{ext}}|$  there is no solution for  $\theta$  in Eq. (1), meaning that  $\hat{m}$  cannot remain in the  $yz$  plane. By solving the full vector equation  $\vec{\tau}_{\text{tot}} = 0$ , we find that for large  $|\tau_{ST}^0|$  there is a current-stabilized regime in which  $\hat{m}$  develops a component in the  $+\hat{x}$  direction for positive  $\tau_{ST}^0$  and  $\hat{m}$  tilts toward  $-\hat{x}$  for negative  $\tau_{ST}^0$ . In our experiments, we have not yet been able to apply large enough steady-state currents to

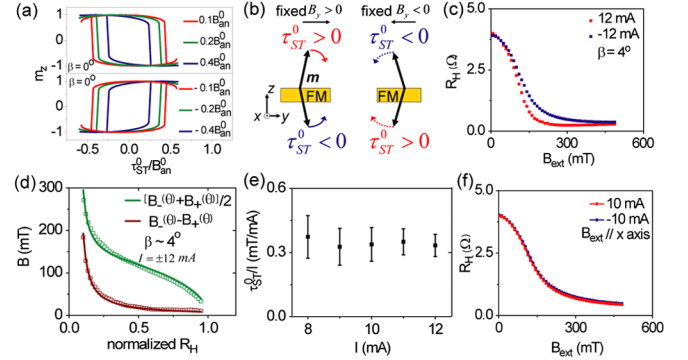


FIG. 2 (color online). (a) Predictions for current-induced magnetic switching within the macrospin model. (b) Illustration of the tilted magnetic states that are stable in the absence of a current when a fixed in-plane magnetic field (left)  $B_y > 0$  or (right)  $B_y < 0$  is applied. The tilt angle is exaggerated compared to Figs. 1(a) and 1(b). Current-induced switching depends on the sign of  $\tau_{ST}^0$  as shown. (c)  $R_H$  vs  $B_{\text{ext}}$ , measured during coherent rotation for  $I = \pm 12$  mA, when the magnetic field is in the  $yz$  plane at  $\beta = 4^\circ$ . (d) Points: measured values of  $B_-(\theta) - B_+(\theta)$  and  $[B_-(\theta) + B_+(\theta)]/2$  as defined in the text, determined from the data in (c). Lines: fits to the macrospin model to determine  $\tau_{ST}^0(I)$  and  $B_{\text{an}}^0(I)$ . (e)  $\tau_{ST}^0/I$  measured for different values of  $I$ . (f)  $R_H$  as a function of the applied field when  $B_{\text{ext}}$  is applied along the  $x$  direction, for  $I = \pm 10$  mA. The curves are indistinguishable, allowing us to set a limit on the in-plane Rashba field.

achieve this state. However, the SHE-induced rotation of  $\hat{m}$  out of the  $yz$  plane predicted in this regime has the correct symmetry to explain observations of stochastic domain reversal in response to large pulsed currents [9], as a possible alternative [25] to the mechanism of large in-plane ( $\pm \hat{x}$ ) Rashba fields proposed by Miron *et al.*

The full switching phase diagram for  $\hat{m}(\tau_{ST}^0, B_y, B_z)$  in the macrospin model can be calculated as described in the Supplementary Material [25]; we illustrate particular sections through the phase diagram in Figs. 3(a) and 3(b).

*Measurements of SHE torque and the Rashba field.*— Before analyzing the experimental switching data, we consider measurements in which the Co magnetic moment rotates coherently. By analyzing the direction and magnitude of current-induced rotation we can distinguish the SHE torque from an in-plane Rashba field [9] and measure the SHE torque.

We first apply  $\vec{B}_{\text{ext}}$  in the  $yz$  plane with a small angle  $\beta = 4^\circ$  relative to the  $y$  axis [Fig. 2(c)]. In this case, the field-induced torque is parallel to  $\hat{x}$  so it adds to or subtracts from the SHE torque, depending on the sign of  $I$ . The nonzero angle  $\beta$  suppresses domain formation so that the magnetization rotates coherently, and the macrospin model applies. We compare field sweeps for the same magnitude of current, positive and negative [ $I = \pm 12$  mA in Fig. 2(c)], so that Ohmic heating should be identical. We define  $B_+(\theta)$

as the value of  $B_{\text{ext}}$  required to produce a given value of  $\theta$  when  $I$  is positive and  $B_-(\theta)$  as the corresponding quantity for  $I$  is negative. From Eq. (1),  $B_{+/-}(\theta) = [B_{\text{an}}^0 \sin\theta \cos\theta \mp \tau_{ST}^0] / \sin(\theta - \beta)$ , so that  $B_-(\theta) - B_+(\theta) = 2\tau_{ST}^0 / \sin(\theta - \beta)$ . The angle  $\beta$  is known for our apparatus with an accuracy of  $\pm 1^\circ$  [25] and  $\sin\theta$  can be determined accurately from  $R_H$ . Therefore, by taking the difference of the two experimental  $B_{\text{ext}}$  versus  $R_H$  curves (for  $\pm I$ ) [Fig. 2(d)] and performing a one-parameter fit, we can determine  $\tau_{ST}^0 = 4.0 \pm 0.7$  mT for  $I = 12$  mA or  $\tau_{ST}^0/I = 0.33 \pm 0.06$  mT/mA. We find that  $\tau_{ST}^0/I$  is approximately independent of  $I$  [Fig. 2(e)]. A current of 12 mA corresponds to a charge current density  $J_e = 2.3 \times 10^7$  A/cm<sup>2</sup>, assuming for simplicity that the current density is uniform throughout the Pt/Co bilayer and the Al is fully oxidized. Using  $\tau_{ST}^0 = \hbar J_S / (2eM_S t)$  with the measured value  $M_S \approx 1.0 \times 10^6$  A/m, our value of  $\tau_{ST}^0$  at 12 mA corresponds to  $J_S \approx 7 \times 10^5$  A/cm<sup>2</sup>, or  $J_S(d = 2 \text{ nm})/J_e = 0.03 \pm 0.01$ . After accounting for a correction associated with the fact that the Pt thickness  $d$  is comparable to the spin diffusion length, this value of  $J_S(d = 2 \text{ nm})/J_e$  corresponds to a bulk value  $J_S(d = \infty)/J_e = 0.06 \pm 0.02$  [25]. This agrees quantitatively with measurements for in-plane-polarized Pt Permalloy bilayers [1,3,26]. A similar analysis of  $B_+(\theta) + B_-(\theta)$  allows a determination of  $B_{\text{an}}^0$  as a function of  $|I|$  [25]:  $B_{\text{an}}^0 = 280$  mT near  $I = 0$  and decreases significantly as a function of increasing  $|I|$ , reflecting heating.

Next we describe a similar experiment with  $\vec{B}_{\text{ext}} = B_x \hat{x}$ . If there is any current-induced Rashba field, it should be primarily in the  $\hat{x}$  direction [27–30], yielding current-induced shifts in  $R_H$  vs  $B_x$  curves. Figure 2(f) shows representative data for  $I = \pm 10$  mA, a current density  $1.9 \times 10^7$  A/cm<sup>2</sup>. We observe no measurable shift between the two curves for any value of  $|I|$ , from which we conclude that any Rashba field in our sample has a magnitude that is less than our sensitivity,  $|B_{\text{Rashba}}|/J_e < 1.3 \times 10^{-7}$  mT/(A/cm<sup>2</sup>). This result is in striking contrast to Ref [9], where an  $\hat{x}$ -oriented Rashba field 75 times larger than our upper bound was reported for similar Pt(30)/Co(6)/AlO<sub>x</sub> samples. [The  $\hat{x}$ -oriented Oersted field, which is  $|B_{\text{Oersted}}|/J_e = \mu_0 d / 2 = 1.3 \times 10^{-8}$  mT/(A/cm<sup>2</sup>) by Ampere's law, is less than our measurement sensitivity.]

*Analysis of experimental switching phase diagrams.*— Representative sections of our measured room-temperature switching phase diagrams (SPDs) are plotted in Figs. 3(c) and 3(d). Qualitatively, these SPDs have shapes and symmetries very similar to the stability boundaries in the macrospin model [Figs. 3(a) and 3(b)], supporting our assertion that the switching can be explained by the SHE-torque. However, to analyze the effects of the SHE-torque quantitatively, it is not appropriate to use a zero-temperature macrospin model for two reasons: (i) current-induced heating can be significant and (ii) magnetic switching occurs by means of a spatially nonuniform reversal process. Nonuniform switching is evident even

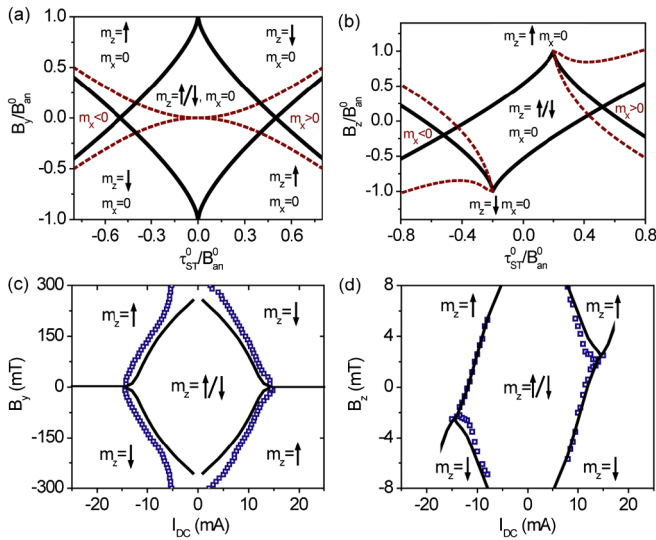


FIG. 3 (color online). (a), (b) SPD calculated in the zero-temperature macrospin model for (a)  $B_{\text{ext}}$  applied along the  $y$  axis and (b)  $B_y$  fixed at  $0.2B_{\text{an}}^0$  with  $B_z$  varied continuously. Switching boundaries for the  $\{m_z = \uparrow / \downarrow, m_x = 0\}$  states (solid lines). Limits of stability for the  $m_x \neq 0$  states (dashed lines). (c), (d) SPD determined experimentally by (c) sweeping  $I$  for fixed values of  $B_{\text{ext}}$  along the  $y$  axis, and (d) fixing  $B_y = 40$  mT and sweeping  $B_z$ . The solid lines in (c) and (d) represent switching boundaries calculated using the modified Stoner-Wohlfarth model. In all panels, the symbol  $\uparrow$  means  $m_z > 0$  and  $\downarrow$  means  $m_z < 0$ , not  $m_z = \pm 1$ .

for  $I = 0$ , in that the easy axis switching field [ $B_c = 17$  mT, see Fig. 1(d)] is much less than the value  $B_c = B_{\text{an}}^0$  expected within the macrospin model ( $B_{\text{an}}^0 = 280$  mT near  $I = 0$ , determined above). Nevertheless, we can achieve a reasonable quantitative modeling of the SPDs by including the effects of the SHE torque within a modified Stoner-Wohlfarth model [31] that accounts approximately for the reduced switching threshold for fields in the  $z$  direction by substituting a reduced perpendicular coercive field  $B_c(|I|)$  in place of  $B_{\text{an}}^0$  [see Eq. (S23) in [25]]. We determine  $B_c(|I|)$  experimentally by measuring the switching field as a function of  $I$  for  $\vec{B}_{\text{ext}}$  perpendicular to the sample plane, the angle for which spin-torque effects are weakest [25]. The only other parameters in the model are the SHE-torque strength  $\tau_{\text{ST}}^0(I) = (0.33 \text{ mT/mA})I$  and  $B_{\text{an}}^0(|I|)$  as determined above. With these inputs, switching currents can be calculated in the modified Stoner-Wohlfarth model for all field values and compared to the experiment with no adjustment of fitting parameters [solid lines in Figs. 3(c) and 3(d)]. We find remarkable agreement considering the simplicity of the model. In particular, the skewed shape of the hysteretic region in Fig. 3(d) is reproduced with no fitting parameters. We conclude that the SHE torque in combination with heating provides a *quantitative* description for the current-driven switching. Heating alone cannot explain the data, since heating depends on  $|I|$  and we measure opposite signs of switching for opposite signs of  $I$ .

Because our measurements of both magnetization rotation and switching are explained quantitatively by the same value of  $J_S/J_e$ , and this number is in agreement with previous experiments, we argue that the SHE-torque mechanism fully explains the current-induced switching, with no evidence for the out-of-plane ( $\pm \hat{z}$ ) Rashba effect proposed in Ref. [11] (see additional discussion in [25]). Theoretical calculations indicate that any Rashba field in the  $\pm \hat{z}$  direction should be accompanied by an even larger Rashba field along  $\pm \hat{x}$  [27–30], so the lack of a measurable  $\pm \hat{x}$  Rashba field in our rotation experiments gives additional reason to question the existence of a large  $\pm \hat{z}$  Rashba field. We have also measured current-induced switching in Pt(30)/Co(5)/Ni(10)/Ta(10) (Fig. S4 in [25]), Pt(30)/Co(5)/Ni(10)/Au(10), and Pt(30)/CoFeB(10)/MgO(16) samples (thicknesses in Å). This shows that the switching does not depend on the presence of an oxide capping layer, and occurs for ferromagnet thicknesses up to 15 Å and for ferromagnets with different chemical compositions. These observations suggest strongly that it is the Pt film which drives switching, rather than a Rashba field within the ferromagnet.

*Ramifications.*—The SHE torque is attractive for applications because, in principle, it can be more efficient than conventional spin torque from spin-polarized currents produced by spin filtering. In a conventional spin-torque device, the efficiency of the torque cannot exceed one unit of

$\hbar/2$  transferred per electron in the current. However, for SHE torque in the geometry of Fig. 1(e), where the charge current flows through a small in-plane area  $a$  and the spin current acts through a much larger perpendicular area  $A$ , the ratio of the total spin current to the total charge current is  $I_S/I_e = J_S A / (J_e a) = (A/a)\theta_{\text{SH}}$ . This can be greater than one even when the spin Hall (SH) angle  $\theta_{\text{SH}} \ll 1$ , meaning that for every electron charge passing through the device many  $\hbar/2$  units of angular momentum can flow perpendicular to the film to apply a spin torque to the magnetic layer.

Understanding that the SHE torque explains current-induced switching of perpendicularly polarized magnetic layers enables quantitative estimates for how to optimize the effect. For a sufficiently small sample, the macrospin model should apply. We assume a magnetic layer of length  $L$ , width  $w$ , and thickness  $t$  for which the perpendicular anisotropy field is optimized to provide an energy barrier of  $40k_B T$  (where  $k_B$  is Boltzmann’s constant and  $T = 300$  K), corresponding to a retention time of 10 yr [32]. The small, fixed, symmetry-breaking in-plane magnetic field needed to set the direction of the spin-Hall switching can be applied easily by the dipole field from a nearby magnetic layer. A simple analysis yields a critical current for SHE switching [25];

$$I_c = \frac{2e(40k_B T)[d + (\sigma_F/\sigma_{\text{Pt}})t]}{\hbar L(J_S(d = \infty)/J_{e,\text{Pt}})[1 - \text{sech}(d/\lambda_{\text{sf}})]} \times \frac{M_S(|I_c|)B_{\text{an}}^0(|I_c|)}{M_S(I = 0)B_{\text{an}}^0(I = 0)}. \quad (2)$$

Here  $d$  is the Pt thickness,  $\sigma_F$  and  $\sigma_{\text{Pt}}$  are the conductivities of the ferromagnet and Pt, and  $\lambda_{\text{sf}}$  is the Pt spin diffusion length. For a sample with  $L = 200$  nm,  $d = 2$  nm,  $t = 0.6$  nm,  $J_S(d = \infty)/J_{e,\text{Pt}} = 0.07$  [3],  $\lambda_{\text{sf}} = 1.4$  nm [21], and assuming for simplicity  $\sigma_F = \sigma_{\text{Pt}}$ , we conclude that  $I_c$  should be  $\sim 170 \mu\text{A}$  even in the absence of any assistance from heating-induced thermal activation. The critical currents would be reduced even further with heating, or by using materials [8] that generate stronger SHE torques. Switching currents for the SHE torque therefore have the potential to be competitive with the optimum switching currents for magnetic tunnel junctions) controlled by conventional spin-transfer torque [32–34]. Compared to conventional magnetic tunnel junctions, spin-Hall switched devices have an advantage that charge currents do not need to flow through tunnel barriers that are sensitive to electrical breakdown.

The SHE torque may also have an important influence on current-driven magnetic domain wall motion in nanowires made from layered heavy-metal–ferromagnet structures, where, e.g., the nonadiabatic torque has been measured to be anomalously strong [35–37].

We acknowledge support from ARO, ONR, DARPA, NSF/MRSEC (DMR-1120296) through the Cornell Center for Materials Research (CCMR), and NSF/NSEC

through the Cornell Center for Nanoscale Systems. We also acknowledge NSF support for T. G. and through use of the Cornell Nanofabrication Facility/NNIN and the CCMR facilities.

- 
- [1] K. Ando, S. Takahashi, K. Harii, K. Sasage, J. Ieda, S. Maekawa, and E. Saitoh, *Phys. Rev. Lett.* **101**, 036601 (2008).
- [2] Y. Kajiwara, K. Harii, S. Takahashi, J. Ohe, K. Uchida, M. Mizuguchi, H. Umezawa, H. Kawai, K. Ando, K. Takanashi, S. Maekawa, and E. Saitoh, *Nature (London)* **464**, 262 (2010).
- [3] L. Q. Liu, T. Moriyama, D. C. Ralph, and R. A. Buhrman, *Phys. Rev. Lett.* **106**, 036601 (2011).
- [4] Z. Wang, Y. Sun, M. Wu, V. Tiberkevich, and A. Slavin, *Phys. Rev. Lett.* **107**, 146602 (2011).
- [5] V. E. Demidov, S. Urazhdin, E. R. J. Edwards, M. D. Stiles, R. D. McMichael, and S. O. Demokritov, *Phys. Rev. Lett.* **107**, 107204 (2011).
- [6] Z. Wang, Y. Sun, Y.-Y. Song, M. Wu, H. Schultheiß, J. E. Pearson, and A. Hoffmann, *Appl. Phys. Lett.* **99**, 162511 (2011).
- [7] E. Padrón-Hernández, A. Azevedo, and S. M. Rezende, *Appl. Phys. Lett.* **99**, 192511 (2011).
- [8] L. Q. Liu, C.-F. Pai, Y. Li, H. W. Tseng, D. C. Ralph, and R. A. Buhrman, *Science* **336**, 555 (2012).
- [9] I. M. Miron, Gilles Gaudin, S. Auffret, B. Rodmacq, A. Schuhl, S. Pizzini, J. Vogel, and P. Gambardella, *Nature Mater.* **9**, 230 (2010).
- [10] U. H. Pi, K. W. Kim, J. Y. Bae, S. C. Lee, Y. J. Cho, K. S. Kim, and S. Seo, *Appl. Phys. Lett.* **97**, 162507 (2010).
- [11] I. M. Miron, K. Garello, G. Gaudin, P.-J. Zermatten, M. V. Costache, S. Auffret, S. Bandiera, B. Rodmacq, A. Schuhl, and P. Gambardella, *Nature (London)* **476**, 189 (2011).
- [12] T. Suzuki, S. Fukami, N. Ishiwata, M. Yamanouchi, S. Ikeda, N. Kasai, and H. Ohno, *Appl. Phys. Lett.* **98**, 142505 (2011).
- [13] M. I. Dyakonov and V. I. Perel, *Phys. Lett.* **35A**, 459 (1971).
- [14] J. E. Hirsch, *Phys. Rev. Lett.* **83**, 1834 (1999).
- [15] S. F. Zhang, *Phys. Rev. Lett.* **85**, 393 (2000).
- [16] J. Sinova, D. Culcer, Q. Niu, N. A. Sinitsyn, T. Jungwirth, and A. H. MacDonald, *Phys. Rev. Lett.* **92**, 126603 (2004).
- [17] S. Murakami, N. Nagaosa, and S. C. Zhang, *Science* **301**, 1348 (2003).
- [18] Y. K. Kato, R. C. Myers, A. C. Gossard, and D. D. Awschalom, *Science* **306**, 1910 (2004).
- [19] S. O. Valenzuela and M. Tinkham, *Nature (London)* **442**, 176 (2006).
- [20] T. Kimura, Y. Otani, T. Sato, S. Takahashi, and S. Maekawa, *Phys. Rev. Lett.* **98**, 156601 (2007).
- [21] L. Q. Liu, R. A. Buhrman, and D. C. Ralph, [arXiv:1111.3702](https://arxiv.org/abs/1111.3702).
- [22] J. Z. Sun and D. C. Ralph, *J. Magn. Magn. Mater.* **320**, 1227 (2008).
- [23] N. Nagaosa, J. Sinova, S. Onoda, A. H. MacDonald, and N. P. Ong, *Rev. Mod. Phys.* **82**, 1539 (2010).
- [24] E. C. Stoner and E. P. Wohlfarth, *Phil. Trans. R. Soc. A* **240**, 599 (1948).
- [25] See Supplemental Material at <http://link.aps.org/supplemental/10.1103/PhysRevLett.109.096602> for details on experimental methods and additional analysis.
- [26] Other values have been reported in the literature for the Pt spin-Hall angle, but we have argued that these variations are due to insufficient (or incorrect) accounting for current shunting, or assumptions regarding the value of the spin diffusion length. For a review, see [21].
- [27] A. Manchon and S. Zhang, *Phys. Rev. B* **78**, 212405 (2008).
- [28] K.-W. Kim, S.-M. Seo, J. Ryu, K.-J. Lee, and H.-W. Lee, *Phys. Rev. B* **85**, 180404(R) (2012).
- [29] X. Wang and A. Manchon, [arXiv:1111.5466](https://arxiv.org/abs/1111.5466).
- [30] D. A. Pesin and A. H. MacDonald, *Phys. Rev. B* **86**, 014416 (2012).
- [31] A. L. Ribeiro, *J. Magn. Magn. Mater.* **133**, 97 (1994).
- [32] J. Z. Sun, *Phys. Rev. B* **62**, 570 (2000).
- [33] T. Kishi, H. Yoda, T. Kai, T. Nagase, E. Kitagawa, M. Yoshikawa, K. Nishiyama, T. Daibou, M. Nagamine, M. Amano, S. Takahashi, M. Nakayama, N. Shimomura, H. Aikawa, S. Ikegawa, S. Yuasa, K. Yakushiji, H. Kubota, A. Fukushima, M. Oogane, T. Miyazaki, and K. Ando, *Proc. IEDM 2008* (IEEE, San Francisco 2008).
- [34] S. Ikeda, K. Miura, H. Yamamoto, K. Mizunuma, H. D. Gan, M. Endo, S. Kanai, J. Hayakawa, F. Matsukura, and H. Ohno, *Nature Mater.* **9**, 721 (2010).
- [35] O. Boulle, J. Kimling, P. Warnicke, M. Kläui, U. Rüdiger, G. Malinowski, H. J. M. Swagten, B. Koopmans, C. Ulysse, and G. Faini, *Phys. Rev. Lett.* **101**, 216601 (2008).
- [36] I. M. Miron, P.-J. Zermatten, G. Gaudin, S. Auffret, B. Rodmacq, and A. Schuhl, *Phys. Rev. Lett.* **102**, 137202 (2009).
- [37] L. San Emeterio Alvarez, K.-Y. Wang, S. Lepadatu, S. Landi, S. J. Bending, and C. H. Marrows, *Phys. Rev. Lett.* **104**, 137205 (2010).